Mechanism and Machine Theory 169 (2022) 104661

Contents lists available at ScienceDirect

Mechanism and Machine Theory

journal homepage: www.elsevier.com/locate/mechmt

Acceleration analysis of 6-RR-RP-RR parallel manipulator with offset hinges by means of a hybrid method

Yang Zhang [a,b], Hasiaoqier Han [a,*], Hui Zhang [a,b], Zhenbang Xu [a,b,*], Yan Xiong [a,b], Kang Han [a], Yaobin Li [a]

[a] Changchun Institute of Optics, Fine Mechanics and Physics, Chinese Academy of Sciences, No.3888, Dong Nanhu Road, Changchun 130033, China
[b] Center of Materials Science and Optoelectronics Engineering, University of Chinese Academy of Sciences, Beijing 100049, China

ARTICLE INFO

Keywords:
Parallel manipulator
Kinematics
Differential transformation method
Velocity analysis
Acceleration analysis

ABSTRACT

In this work, the kinematics of a symmetrical hexapod parallel manipulator is investigated by means of Denavit-Hartenberg method and differential transformation method. When compared with a general Gough-Stewart platform, the limbs of the parallel manipulator are connected to the mobile and fixed platforms through offset hinges, rather than traditional spherical and universal hinges. Because the offset variable of the hinge axis are introduced by the offset hinge, the kinematics of the parallel manipulator studied becomes more complicated. The forward and inverse displacement analysis are approached by means of the Denavit-Hartenberg method. Then, the velocity and acceleration are analyzed using differential transformation method. The concise expression is obtained and can be easily translated into computer program. The derivation of acceleration analysis of the 6-RR-RP-RR parallel manipulator using the hybrid approach is novel in this research field. Finally, a numerical example is given and the numerical results are verified via co-simulation.

1. Introduction

When compared with the serial manipulator, the parallel manipulator usually has advantages including high precision, high rigidity and large bearing capacity, attracting researchers' extensive interest and promoting the rapid development of parallel manipulators. We need to especially thank Gough and Stewart for their pioneering contributions in the field of parallel manipulators. Gough [1,2] designed a tire testing machine in 1947. It has six degrees of freedom and can adjust the position and direction of tires installed on the platform. It is the earliest known Hexapod parallel robot. Stewart [3,4] proposed the concept of a six-DOF flight simulator motion model in 1965. Although the structures of the devices proposed by them are different, the six-legged parallel manipulators are commonly referred to Gough-Stewart platforms. A typical Gough-Stewart platform, as shown in Fig. 1, consists of a mobile platform, a fixed platform and six driving legs of adjustable length. The ends of all legs are connected to the mobile and fixed platform through spherical and universal hinges (or both spherical hinges, both universal hinges). In recent decades, there are many interesting inventions for parallel robots in many fields, including manufacturing, precision positioning, and motion simulators. Moreover, hexapod parallel robots have been used widely, including motion simulators [5–9], vibration isolation systems based on

* Corresponding authors at: Changchun Institute of Optics, Fine Mechanics and Physics, Chinese Academy of Sciences, No.3888, Dong Nanhu Road, Changchun 130033, China.
E-mail addresses: hanhasiaoqier@yahoo.com (H. Han), xuzhenbang@ciomp.ac.cn (Z. Xu).

https://doi.org/10.1016/j.mechmachtheory.2021.104661
Received 19 January 2021; Received in revised form 15 October 2021; Accepted 16 November 2021
Available online 4 December 2021

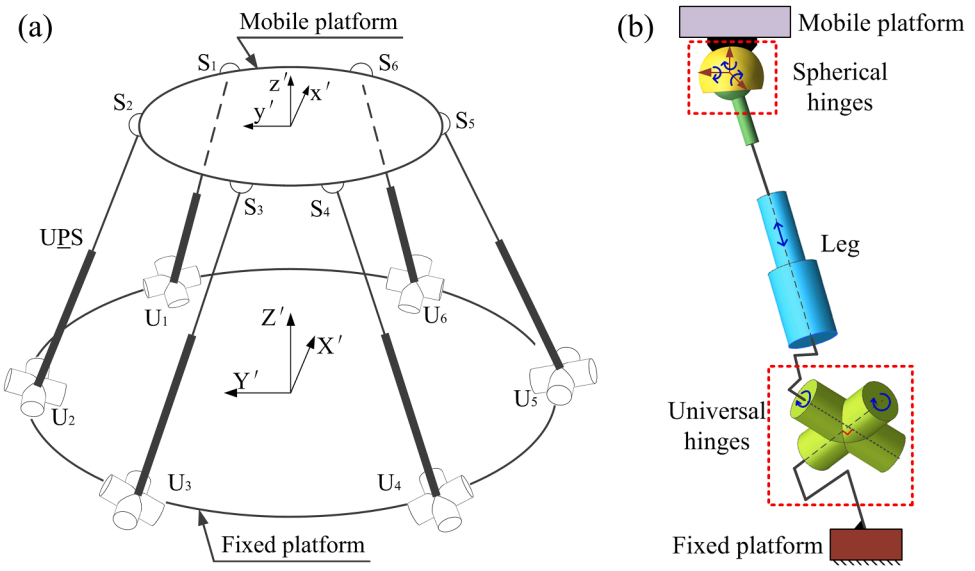

Fig. 1. The traditional Gough-Stewart parallel manipulator: (a) The diagram of the mechanism; (b) The UPS kinematic chain.

Stewart mechanisms [10–12], parallel mechanisms for precise pointing of telescopes [13–15], six-dimensional force sensors [16–18], and cable-driven parallel robots [19,20]. Parallel robots with fewer DOFS have also been applied increasingly, including machine tools [21–25], Delta parallel robots achieving high-speed pick-and-place operation [26–29] in the industrial field, and the medical surgery [30,31].

In recent years, the theoretical research of parallel manipulators has also made great progress, including the forward and inverse kinematics. For the parallel manipulator with fewer degrees of freedom, the kinematics is relatively simple because it is partially decoupled or completely decoupled, and generally has analytical solutions. Gallardo-Alvarado et al. [32–34] used the screw theory to obtain the kinematics analytical solution for 4-DOF CPS-PS-HPS parallel manipulator, 3-DOF SP-SPR-SPS parallel manipulator and 2SPS-RPS-PS parallel manipulator, respectively. And numerical examples were given for verification. For a general Gough-Stewart platform, such as 6-UPS [35], 6-SPS [36] and 6-UCU [37], its kinematics has analytical solutions. Although the forward displacement analysis is more complicated, it has been studied widely. When a set of generalized coordinates are given, the mobile platform can reach 40 different postures [38,39]. U, P, S, C, R, H denote a universal hinge, a prismatic hinge, a spherical hinge, a cylindrical hinge, a revolute hinge, a Hooke hinge, respectively. Rolland [40] introduced an accurate algebraic method to solve the forward kinematics problem of hexapod robots, and gave eight real solutions for several different hexapod robots. Gallardo Alvarado [41] solved the forward displacement analysis of a general 6-6 parallel manipulator based on generating a closed equation on the unknown coordinates of three points embedded in the mobile platform. Gan [42] used Gröbner basis theory to simplify the forward displacement problem of the general 6-6 Stewart mechanism into a 40-degree polynomial equation, and constructed Sylvester's matrix to derive 40 different positions of the mobile platform. Huang [43] simplified the forward kinematics of a symmetric 6-6 Stewart platform into a 14-degree univariate polynomial equation using a concise algebraic elimination algorithm, and obtained all closed form solutions of forward kinematics. Although the general Gough-Stewart platform has been used successfully, its performances including workspace and rigidity are restricted by hinges. Traditional universal hinges and spherical hinges have problems including low rigidity, small workspace, and easy to produce manufacturing and installation errors. Therefore, different types of hinges have been studied to replace traditional hinges. Hu et al. [44] analyzed the the workspace of an offset 3-RRPRR parallel manipulator. The 3-RRPRR configuration with offset hinges has a larger reachable workspace than its similar structure 3-RRPU, 3-RPRU, 3-UPU. Gloess et al. [45] designed an offset universal hinge with rigidity of up to twice that of a conventional universal hinge to meet the high rigidity and high load requirements of parallel platforms. The designs of this type of hinge require fewer components and can be manufactured more accurately. Großmann et al [46] discussed three possible types of eccentric universal hinges as an alternative to traditional universal hinges. Such an eccentric design makes pivoting range of hinge larger. The two hinge axes of the offset universal hinge [44–46] are perpendicular to each other but do not intersect, thus it is easy to manufacture, and can provide higher rigidity and larger rotation space. However, the offset hinge introduces the offset variable between the hinge axes, making the kinematics more complicated than that of the general parallel mechanism using traditional hinges. Moreover, this kind of kinematics is difficult to solve effectively and there is no analytical solution. The kinematics methods for the general parallel mechanism are no longer applicable. Dalvand and Shirinzadeh [47,48] studied the kinematics of 6-RRCRR parallel manipulators with offset hinges, and proposed a hinge constraint algorithm to solve it. Via the same method, Yu [49] studied the kinematics of 6-RR-RP-RR parallel manipulator with similar configuration, and Han [50] studied the kinematics of 6-P-RR-R-RR parallel manipulator. And P, C and RP denote an actuated prismatic joint, an actuated cylindrical joint, and an actuated ball screw pair, respectively. RP joint is similar to C joint.

However, the above method has great limitations, and the modeling process is complicated. Moreover, it can only be used for

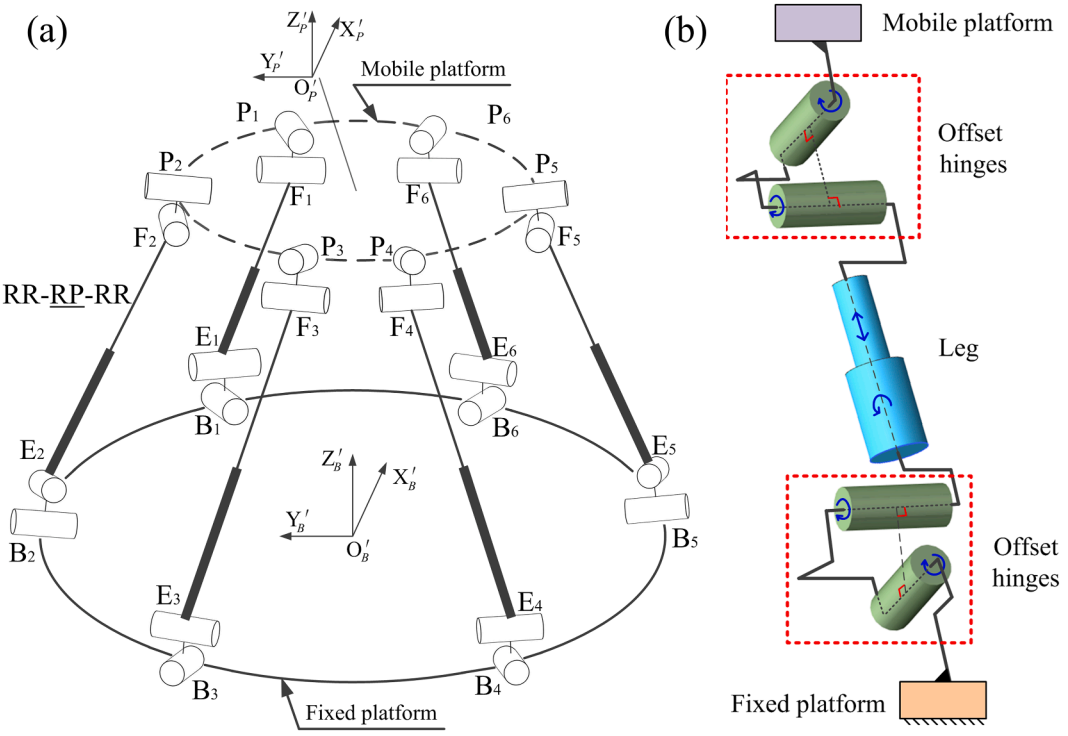

Fig. 2. The parallel manipulator under study: (a) The diagram of the mechanism; (b) The RR-RP-RR kinematic chain.

displacement analysis, and cannot analyze the velocity and acceleration of the parallel mechanism. In order to realize the real-time tracking of the trajectory and attitude of the spacecraft and other targets, in response to the needs of the large-aperture ground-based telescope for the dynamic adjustment of the position and attitude of the secondary mirror and the precise tracking and positioning, the 6-RR-RP-RR six-degree-of-freedom parallel manipulator with high accuracy, high rigidity and large working stroke is studied and applied to the secondary mirror adjustment system of the large-aperture ground-based telescope. The secondary mirror system requires high precision, high rigidity and large working stroke. The general Gough-Stewart manipulator has the problems of limited workspace and low rigidity. To improve these shortcomings, the offset hinges are introduced to improve the workspace and rigidity of the parallel manipulator. Because the secondary mirror system needs to realize the dynamic adjustment of position and attitude and the precise tracking and positioning, it is necessary to analyze the velocity and acceleration of the parallel manipulator. The velocity and acceleration analysis of the Gough-Stewart parallel manipulator using offset hinges has not been reported in previous studies. In order to fill this gap, this contribution successfully uses differential transformation method combined with Denavit- Hartenberg parameter method to solve the velocity and acceleration problems of such parallel manipulator. Hybrid methods overcome the limitations of the hinge constraint algorithm, and the modeling process is simple. They lay the foundation for the subsequent dynamic analysis.

In this work, the kinematics of a complex 6-DOF parallel manipulator using offset hinges, known as the 6-RR-RP-RR manipulator, was studied by means of a hybrid method, including the analysis of displacement, velocity and acceleration. This paper is organized as follows. In Section 2, the parallel manipulator studied is described. And the influence of the offset hinge on workspace is verified by an example. In Section 3, the Denavit-Hartenberg parameter method is used for displacement analysis. As far as the authors know, this method is practical and efficient for such parallel manipulator. In Section 4, the velocity and acceleration of the studied parallel manipulator are analyzed via the differential transformation method. A concise expression of the velocity and acceleration of the parallel manipulator was obtained, and this work has not been reported before. In Section 5, a numerical example is given to verify the effectiveness of hybrid methods. Finally, Section 6 summarizes the full text.

2. Description of the mechanism

2.1. Comparison of two parallel manipulators

The parallel manipulator under study is shown in Fig. 2. It consists of a mobile platform, a fixed platform and six symmetrical limbs. Each limb has two links connected to each other by means of a RP joint, and two offset universal hinges (known as RR-hinge) connecting the limb to the mobile and fixed platforms. RP joints play the role of active joints. The main distinction from the traditional Gough-Stewart parallel manipulator is the different hinges used. The traditional Gough-Stewart manipulator, using the spherical

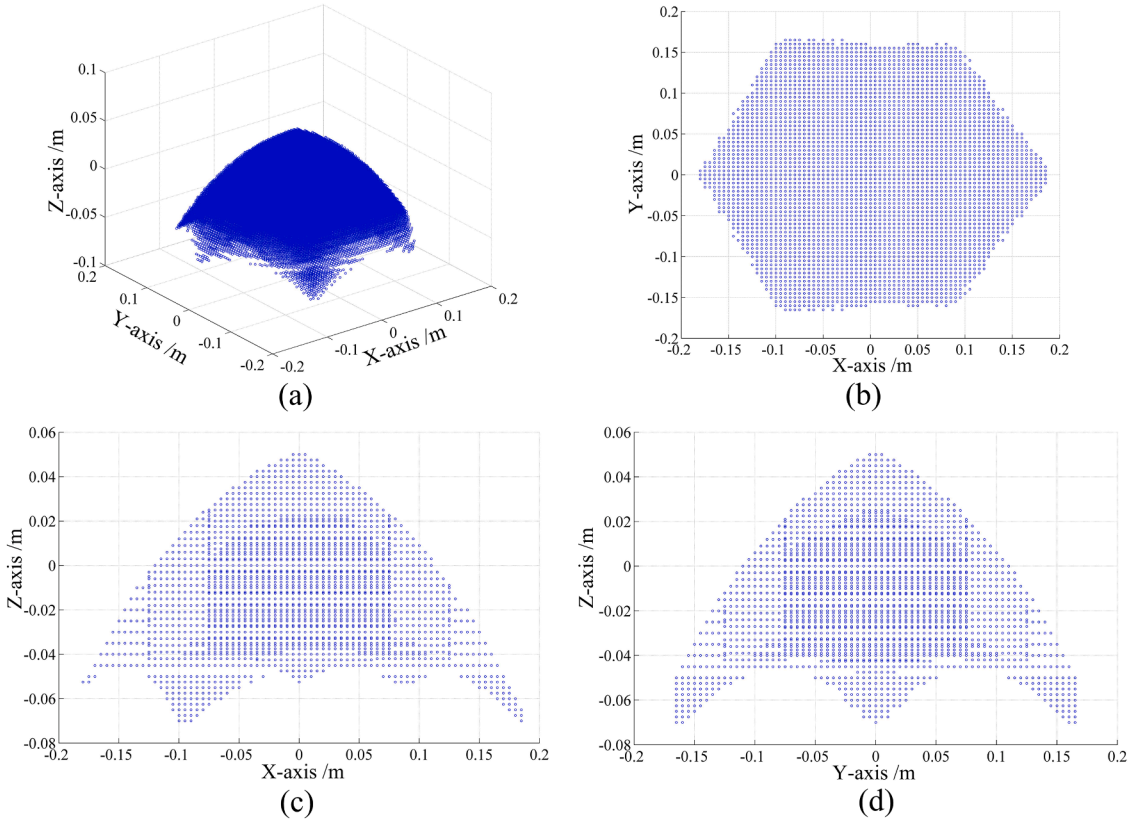

Fig. 3. The positional workspace of the 6-RR-RP-RR parallel manipulator in the initial attitude: (a) Three-dimensional graph; (b) Workspace projection in the X-Y plane; (c) Workspace projection in the X-Z plane;(d) Workspace projection in the Y-Z plane.

hinges, revolute hinges or universal hinges, is relatively simple, with the length of limbs represented in a very simple, intuitive way, as shown in Fig. 1. Points S_i are the centers of the spherical hinges mounted on the mobile platform and located by position vectors $\mathbf{S}_i$. Points U_i are the centers of the universal hinges mounted on the fixed platform and located by position vectors $\mathbf{U}_i$. In the remainder of the contribution, i=1, 2,…, 6. The length of limbs can be expressed as $L_i = (\mathbf{S}_i - \mathbf{U}_i) \cdot (\mathbf{S}_i - \mathbf{U}_i)$. Obviously vectors $\mathbf{S}_i$ and $\mathbf{U}_i$ are easily computed.

However, the parallel manipulator studied in this paper has a much more complex representation of the limb length because the two rotational axes of the offset hinges do not intersect and have a specific offset in space, as shown in Fig. 2. Points E_i and F_i are the centers of the two hinge axes directly connected to limbs, respectively. And they are located by position vectors $\mathbf{E}_i$ and $\mathbf{F}_i$, respectively. The length of limbs can be expressed as $L_i = (\mathbf{F}_i - \mathbf{E}_i) \cdot (\mathbf{F}_i - \mathbf{E}_i)$. However, the vectors $\mathbf{E}_i$ and $\mathbf{F}_i$, having no fixed positional relationship with the mobile platform and fixed platform, are difficult to solve, so the conventional calculation method of the limb length cannot be realized. The solution of its kinematics is a complex task due to offset variable of the offset hinges. We have to find an effective method to solve the kinematics problem of the parallel manipulator under study.

All six limbs are an offset universal + cylindrical + offset universal (RR-C-RR type) kinematic chain. Since the cylindrical joints, usually driven using ball screw pairs, provide two degrees of freedom, the RR-C-RR kinematic chain can be expressed as the RR-RP-RR kinematic chain. This equivalence is mainly to facilitate kinematic modeling of a single limb. According to a revised version of the Kutzbach-Grübuler formula, the manipulator under study possesses six degrees of freedom.

2.2. *Workspace difference between two parallel manipulators*

The offset hinges [44,46] are can provide larger rotation space than traditional hinges. In order to more intuitively verify the influence of the offset hinges on the workspace of the parallel manipulator, the positional workspace of the parallel manipulator under the initial attitude is solved by inverse displacement solution of Section 3.2. The positional workspace refers to the space consisting of all the positions that can be reached by the reference point of the mobile platform under the condition of a given attitude of mobile platform. The positional workspace of two parallel manipulators 6-RR-RP-RR and 6-SPS is analyzed in the fixed initial attitude, and the three-dimensional graphs of the positional workspace are drawn respectively. The two parallel manipulators use the same configuration parameters, as shown in Table 2, and their actuator length limits are the same. The rotation angle constraint of the offset hinges can be solved by establishing an accurate mathematical model [51]. As can be seen from Figs. 3 and 4, the positional workspace of the

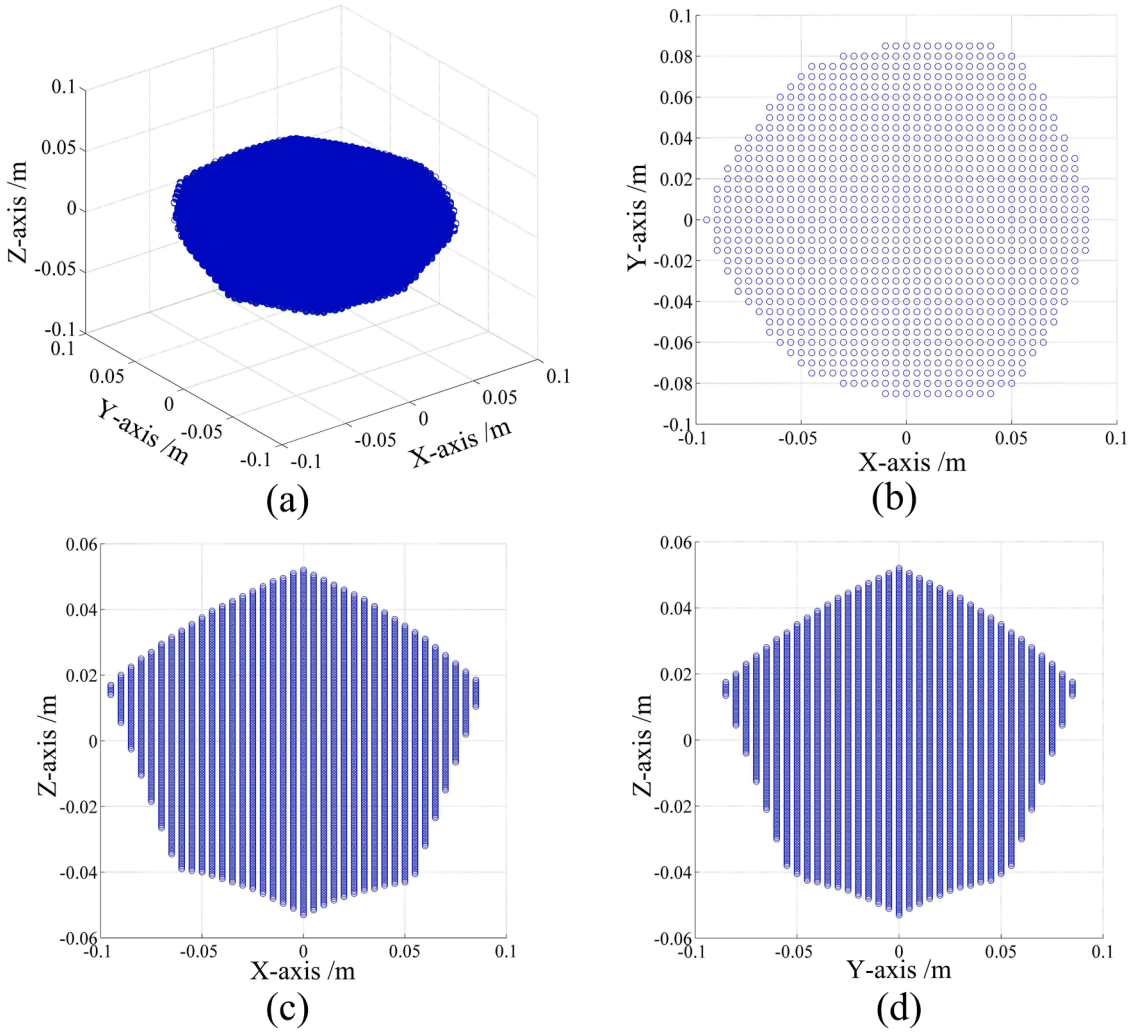

Fig. 4. The positional workspace of the 6-SPS parallel manipulator in the initial attitude: (a) Three-dimensional graph; (b) Workspace projection in the X-Y plane; (c) Workspace projection in the X-Z plane;(d) Workspace projection in the Y-Z plane.

6-RR-RP-RR parallel manipulator with offset hinges is significantly larger than that of the 6-SPS parallel manipulator with spherical hinges. The positional workspace of the 6-SPS parallel manipulator is completely a subspace of the positional workspace of the 6-RR-RP-RR parallel manipulator. Obviously, the offset hinges has a larger rotation range than the spherical hinges and can increase the workspace of the parallel manipulator. Owing to the limitation of space, the singularity analysis will not be presented, and readers can use this approach [52] considering motion/force transmissibility for singularity analysis of parallel manipulators to analyze the singularities of the parallel manipulator.

3. Finite kinematics of the parallel manipulator

In this section the displacement analysis of the parallel manipulator is presented.

3.1. *Kinematics of the i_{th} limb*

Each limb is equivalent to an RR-RP-RR serial manipulator, and the local reference frames established in the limb are depicted in Fig. 5. For the convenience of analysis, the two offset universal hinges connected to each limb are taken as the same. Points P_i are the centers of the hinge axe connected to the mobile platform and located by position vectors $\mathbf{P}_i$. Points B_i are the centers of the hinge axe connected to the fixed platform and located by position vectors $\mathbf{B}_i$. Points E_i and F_i are the centers of the two hinge axes directly connected to limbs, located by position vectors $\mathbf{E}_i$ and $\mathbf{F}_i$, respectively. The origins of the local reference frames coincide with the above four points, respectively. The Denavit-Hartenberg parameters of the i_{th} limb are as shown in Table 1. U_{offset} represents the offset variables of offset universal hinges, that is, the distance between the hinge axes. L_{4i} represents the limb length, that is, the distance

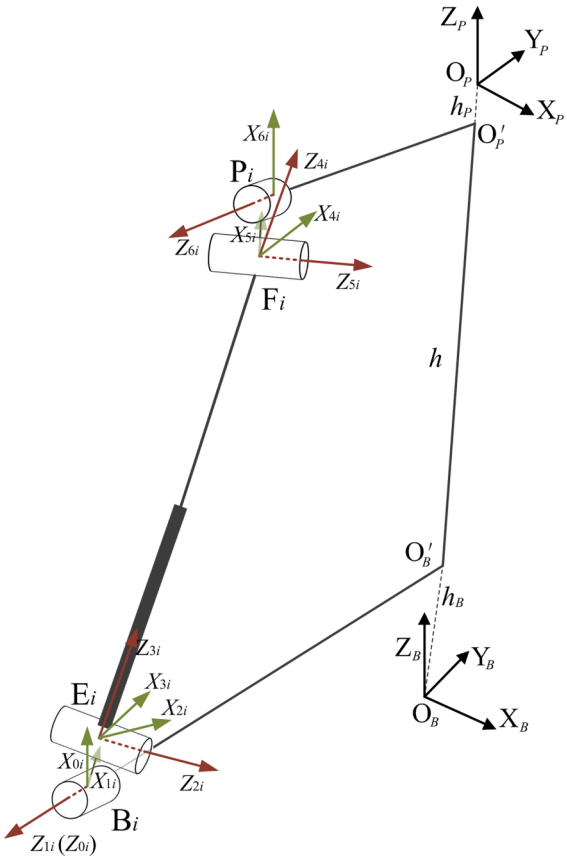

Fig. 5. The local reference frames of the i_{th} actuator limb of the parallel manipulator.

Table 1.
Denavit-Hartenberg parameters of the i_{th} limb.

Link j	θ_{ji}(°)	$\alpha_{(j-1)i}$(°)	d_{ji}(m)	$a_{(j-1)i}$(m)
1	θ_{1i}	0	0	0
2	θ_{2i}	90	0	U_{offset}
3	θ_{3i}	-90	0	0
4	0	0	L_{4i}	0
5	θ_{5i}	90	0	0
6	θ_{6i}	-90	0	U_{offset}

between coordinate axis Z_{2i} and Z_{5i}.

The transformation matrix between two adjacent local reference frames is:

$$^{n}\mathbf{T}_{n+1} = Rot\,(x, \alpha_n) \cdot Trans\,(a_n,\, 0,\, 0) \cdot Rot\,(z, \theta_{n+1}) \cdot Trans\,(0,\, 0,\, d_{n+1}) \tag{1}$$

For the i_{th} limb, the homogeneous transformation matrix of joint n to the end joint can be computed:

$$^{n}\mathbf{T}_{6} = {}^{n}\mathbf{T}_{n+1} \cdot {}^{n+1}\mathbf{T}_{n+2} \cdots {}^{5}\mathbf{T}_{6} \tag{2}$$

3.2. Inverse displacement analysis

The inverse displacement analysis is to find out the length of each limb for the parallel manipulator, given the position and orientation of the mobile platform with respect to the fixed platform. The global reference frame $O'_B - X'_B Y'_B Z'_B$ is attached at the fixed platform and the body reference frame $O'_P - X'_P Y'_P Z'_P$ is attached at the mobile platform, as shown in Fig. 2. In practical application, the mobile platform is to drive the load placed on its upper surface to move. In general, from the perspective of the actual manipulator, both the mobile and fixed platforms have a certain thickness, and the mobile platform motion refers to the motion of the upper surface

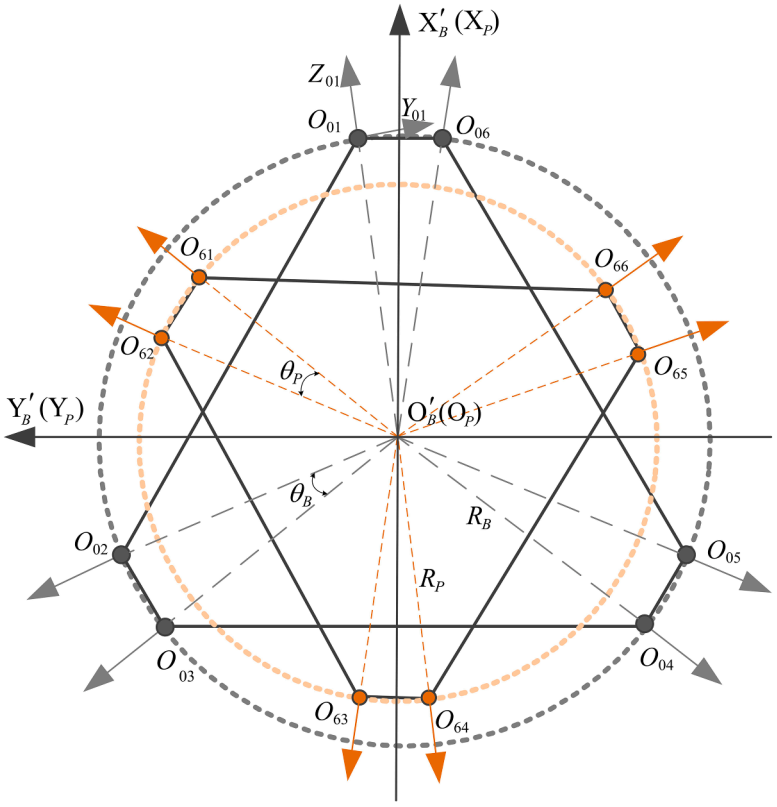

Fig. 6. Layout of hinge center points connected to the platform.

for the mobile platform relative to the lower surface for the fixed platform. Therefore, it is necessary to establish the general body reference frame $O_P - X_P Y_P Z_P$ on the upper surface for the mobile platform and the general global reference frame $O_B - X_B Y_B Z_B$ on the lower surface for the fixed platform, see Fig. 5. The distance between the origin of $O_P - X_P Y_P Z_P$ and the origin of $O'_P - X'_P Y'_P Z'_P$ is h_P, and the distance between the origin of $O_B - X_B Y_B Z_B$ and the origin of $O'_B - X'_B Y'_B Z'_B$ is h_B. The layout of hinge center points P_i and B_i (i=1, …,6) are shown in Fig 6. The origin O_{0i} of the local reference frame $O_{0i} - X_{0i} Y_{0i} Z_{0i}$ is coincident with point B_i, and the origin O_{6i} of the local reference frame $O_{6i} - X_{6i} Y_{6i} Z_{6i}$ is coincident with point P_i. The hinge center points P_i and B_i are respectively distributed on a symmetrical hexagon.

In Section 2, the complexity of the parallel manipulator studied in this paper, due to the use of offset universal hinges, is analyzed and compared. Therefore, the Denavit-Hartenberg parameter method is used to solve the complex kinematics problem, when the conventional methods are ineffective.

In the i_{th} actuator limb as shown in the section 3.1, the pose vector $\overrightarrow{B_i P_i}$ of the end joint for the limb with respect to the reference frame $O_{0i} - X_{0i} Y_{0i} Z_{0i}$ of the limb can be expressed as the following vector chain:

$$\overrightarrow{B_i P_i} = \overrightarrow{B_i E_i} + \overrightarrow{E_i F_i} + \overrightarrow{F_i P_i} = \overrightarrow{B_i O'_B} + \overrightarrow{O'_B O'_P} + \overrightarrow{O'_P P_i} \tag{3}$$

The pose vector $\overrightarrow{B_i P_i}$ can be described by the homogeneous transformation matrix ${}^{0}\mathbf{T}_6$ or the transformation matrix ${}^{0i}\mathbf{T}_{6i}$ of the end joint 6 (coinciding with point P_i) with respect to the reference frame $O_{0i} - X_{0i} Y_{0i} Z_{0i}$. ${}^{0}\mathbf{T}_6$ can be obtained from equation (2), and ${}^{0i}\mathbf{T}_{6i}$ can be obtained when given the pose of the mobile platform in the reference frame $O_B - X_B Y_B Z_B$.

Given the pose vector $\mathbf{q} = [X, Y, Z, \alpha, \beta, \gamma]$ of the frame $O_P - X_P Y_P Z_P$ in the frame $O_B - X_B Y_B Z_B$, the homogeneous transformation matrix ${}^{O_B}\mathbf{T}_{O_P}$ of the mobile platform with respect to the fixed platform can be computed as follows:

$${}^{O_B}\mathbf{T}_{O_P} = \begin{bmatrix} c\beta c\gamma & -c\beta s\gamma & s\beta & X \\ c\alpha s\gamma + s\alpha s\beta c\gamma & c\alpha c\gamma - s\alpha s\beta s\gamma & -s\alpha c\beta & Y \\ s\alpha s\gamma - c\alpha s\beta c\gamma & s\alpha c\gamma + c\alpha s\beta s\gamma & c\alpha c\beta & Z \\ 0 & 0 & 0 & 1 \end{bmatrix} \tag{4}$$

Where, $c\alpha = \cos(\alpha)$, $s\alpha = \sin(\alpha)$, the expressions of β and γ are similar.

The homogeneous transformation matrix ${}^{O_B}\mathbf{T}_{O_{0i}}$ of the local reference frame $O_{0i} - X_{0i} Y_{0i} Z_{0i}$ with respect to the general global

reference frame $O_B - X_B Y_B Z_B$ is as follows:

$$ {}^{O_B}\mathbf{T}_{O_{0i}} = \begin{bmatrix} {}^{O_B}\mathbf{R}_{O_{0i}} & {}^{O_B}\boldsymbol{O}_{0i} \\ \mathbf{0} & 1 \end{bmatrix} \tag{5} $$

where ${}^{O_B}\boldsymbol{O}_{0i}$ is the position vector of point O_{0i} with respect to the reference frame $O_B - X_B Y_B Z_B$, and ${}^{O_B}\mathbf{R}_{O_{0i}}$ is the rotation matrix of the reference frame $O_{0i} - X_{0i} Y_{0i} Z_{0i}$ with respect to the reference frame $O_B - X_B Y_B Z_B$.

The homogeneous transformation matrix ${}^{O_P}\mathbf{T}_{O_{6i}}$ of the local reference frame $O_{6i} - X_{6i} Y_{6i} Z_{6i}$ with respect to the general body reference frame $O_P - X_P Y_P Z_P$ is as follows:

$$ {}^{O_P}\mathbf{T}_{O_{6i}} = \begin{bmatrix} {}^{O_P}\mathbf{R}_{O_{6i}} & {}^{O_P}\boldsymbol{O}_{6i} \\ \mathbf{0} & 1 \end{bmatrix} \tag{6} $$

where ${}^{O_P}\boldsymbol{O}_{6i}$ is the position vector of point O_{6i} with respect to the reference frame $O_P - X_P Y_P Z_P$, and ${}^{O_P}\mathbf{R}_{O_{6i}}$ is the rotation matrix of the reference frame $O_{6i} - X_{6i} Y_{6i} Z_{6i}$ with respect to the reference frame $O_P - X_P Y_P Z_P$.

Therefore, the transformation matrix ${}^{0i}\mathbf{T}_{6i}$ is computed as follows:

$$ {}^{0i}\mathbf{T}_{6i} = \left({}^{O_B}\mathbf{T}_{O_{0i}}\right)^{-1} \cdot {}^{O_B}\mathbf{T}_{O_P} \cdot {}^{O_P}\mathbf{T}_{O_{6i}} \tag{7} $$

For the convenience of expression, ${}^{0i}\mathbf{T}_{6i}$ is abbreviated as

$$ {}^{0i}\mathbf{T}_{6i} = \begin{bmatrix} n_x & r_x & a_x & p_x \\ n_y & r_y & a_y & p_y \\ n_z & r_z & a_z & p_z \\ 0 & 0 & 0 & 1 \end{bmatrix} \tag{8} $$

According to Eq. (3), it can be concluded that:

$$ {}^{0}\mathbf{T}_{6} = {}^{0i}\mathbf{T}_{6i} \tag{9} $$

It can be seen from Eq. (9) that corresponding elements in transformation matrix ${}^{0}\mathbf{T}_{6}$ and ${}^{0i}\mathbf{T}_{6i}$ are equal, so kinematic equations can be established and shown in the Appendix A.

The kinematic equations are all nonlinear equations and contain many variables, thus the analytical solutions can not be obtained. Therefore, the Newton-Raphson iteration method is constructed to solve for nonlinear equations.

3.3. Forward displacement analysis

The forward displacement analysis consists of finding the coordinates of the pose $\mathbf{q} = [X, Y, Z, \alpha, \beta, \gamma]$ for the mobile platform with respect to the fixed platform, given a set of the limb lengths, $L_{4i} (i = 1, \ldots, 6)$.

The forward displacement analysis of the parallel manipulator is more complex than inverse displacement analysis. There are no analytical solutions for the forward displacement analysis and it is solved via numerical methods. The forward displacement analysis will be solved on the basis of inverse displacement analysis.

For a set of the known limb lengths $\boldsymbol{L}_k = [L_{41-k}, L_{42-k}, \cdots, L_{46-k}]^T$, $f(\mathbf{q})$ is obtained as follows:

$$ f(\mathbf{q}) = IPA(\mathbf{q}) - \boldsymbol{L}_k \tag{10} $$

where, $IPA(\mathbf{q})$ is a set of the limb lengths for the parallel manipulator given the pose $\mathbf{q}$ of the mobile platform with respect to the fixed platform.

The Newton-Raphson iteration method can be used to solve Eq. (10). A iterative equation can be obtained as follows

$$ \mathbf{q}_{n+1} = \mathbf{q}_n - \left(\partial f(\mathbf{q}_n)/\partial \mathbf{q}\right)^{-1} \cdot f(\mathbf{q}_n) \tag{11} $$

4. Infinitesimal kinematics of the parallel manipulator

4.1. Velocity analysis

Fig. 5 shows the RR-RP-RR manipulator, where RR and RP denote an offset universal hinge and a ball screw pair, respectively. The ball screw pair contains two movements of rotation and translation, which is equivalent to two joints. Six such manipulators will be used as the connector chains of a parallel manipulator, and the ball screw pair in each connector chain will be actuated. The mathematical tool to approach the infinitesimal kinematics of the parallel manipulator under study is the differential transformation method, and the modeling is depicted in Fig. 5.

The linear mapping relationship between the velocity of manipulator operation space and the velocity of joints is called Jacobi matrix, also known as the first-order influence coefficient matrix. Before studying Jacobi matrix, the differential motion relationship

between two reference frames is analyzed.

Given the reference frame {**T**}, its differential motion in the base reference frame is expressed as$\mathbf{M} = [\mathbf{d}, \quad \boldsymbol{\delta}]^T$, where the differential translation vector is $\mathbf{d} = [d_x,\ d_y,\ d_z]^T$ and the differential rotation vector is $\boldsymbol{\delta} = [\delta_x,\ \delta_y,\ \delta_z]^T$.

The differential motion transformation of {**T**} with respect to the base reference frame can be described as follows:

$$\mathbf{T} + d\mathbf{T}_B = Trans(d_x,\ d_y,\ d_z) \bullet Rot(\mathbf{f},\ d\theta) \bullet \mathbf{T} \tag{12}$$

where, $Trans(d_x,\ d_y,\ d_z)$ represents the differential translation transformation in the base reference frame;

$Rot(\mathbf{f},\ d\theta)$ is the differential rotation transformation for differential rotation $d\theta$ around vector **f** in the base reference frame.

The differential transformation $d\mathbf{T}_B = [Trans(d_x,\ d_y,\ d_z) \bullet Rot(\mathbf{f},\ d\theta) - \mathbf{I}] \bullet \mathbf{T}$ can be obtained from equation (12).

The differential transformation operator is expressed as $\Delta = Trans(d_x,\ d_y,\ d_z) \bullet Rot(\mathbf{f},\ d\theta) - \mathbf{I}$, then the differential transformation $d\mathbf{T}_B$ can be written as follows:

$$d\mathbf{T}_B = \Delta \cdot \mathbf{T} \tag{13}$$

Similarly, the differential motion of the reference frame {$\boldsymbol{T}$} with respect to its own reference frame is ${}^T\mathbf{M} = [{}^T\mathbf{d}, \quad {}^T\boldsymbol{\delta}]^T$, where the differential translation vector is ${}^T\mathbf{d} = [{}^Td_x,\ {}^Td_y,\ {}^Td_z]^T$ and the differential rotation vector is ${}^T\boldsymbol{\delta} = [{}^T\delta_x,\ {}^T\delta_y,\ {}^T\delta_z]^T$.

The differential motion transformation of {**T**} with respect to its own reference frame is given by:

$$d\mathbf{T}_O = \mathbf{T} \bullet \left[Trans\left({}^Td_x,\ {}^Td_y,\ {}^Td_z\right) \bullet Rot\left({}^T\mathbf{f},\ d\theta_T\right) - \mathbf{I}\right] \tag{14}$$

The differential transformation operator is described as ${}^T\Delta = Trans({}^Td_x,\ {}^Td_y,\ {}^Td_z) \bullet Rot({}^T\mathbf{f},\ d\theta_T) - \mathbf{I}$, then the differential transformation $d\mathbf{T}_O$ can be written as follows:

$$d\mathbf{T}_O = \mathbf{T} \cdot {}^T\Delta \tag{15}$$

The derivation of the differential transformation operator Δ is given in the Appendix B, composed of elements in differential motion **M**, and it can be calculated as follows:

$$\Delta = \begin{bmatrix} 0 & -\delta_z & \delta_y & d_x \\ \delta_z & 0 & -\delta_x & d_y \\ -\delta_y & \delta_x & 0 & d_z \\ 0 & 0 & 0 & 0 \end{bmatrix} \tag{16}$$

Similarly, the expression of ${}^T\Delta$ can be obtained:

$${}^T\Delta = \begin{bmatrix} 0 & -{}^T\delta_z & {}^T\delta_y & {}^Td_x \\ {}^T\delta_z & 0 & -{}^T\delta_x & {}^Td_y \\ -{}^T\delta_y & {}^T\delta_x & 0 & {}^Td_z \\ 0 & 0 & 0 & 0 \end{bmatrix} \tag{17}$$

When differential transformation $d\mathbf{T}_B$ of {**T**} with respect to the base reference frame is equivalent to differential transformation $d\mathbf{T}_O$ of {**T**} with respect to its own reference frame, the equation $\Delta \cdot \mathbf{T} = \mathbf{T} \cdot {}^T\Delta$ can be obtained. Then the transformation between two differential operators follows that $\mathbf{T}^{-1} \cdot \Delta \cdot \mathbf{T} = {}^T\Delta$.

The reference frame {**T**} can be written as follows:

$$\mathbf{T} = \begin{bmatrix} n_x & o_x & a_x & p_x \\ n_y & o_y & a_y & p_y \\ n_z & o_z & a_z & p_z \\ 0 & 0 & 0 & 1 \end{bmatrix} \tag{18}$$

Where, **n**, **o**, **a**, **p** are the four column vectors of **T**, such as $\mathbf{n} = [n_x,\ n_y,\ n_z]^T$.

From equations (18) and (B.3), it can be concluded that:

$$\begin{cases} {}^Td_x = \mathbf{n} \cdot ((\boldsymbol{\delta} \times \mathbf{p}) + \mathbf{d}) \\ {}^Td_y = \mathbf{o} \cdot ((\boldsymbol{\delta} \times \mathbf{p}) + \mathbf{d}) \\ {}^Td_y = \mathbf{a} \cdot ((\boldsymbol{\delta} \times \mathbf{p}) + \mathbf{d}) \\ {}^T\delta_x = \mathbf{n} \cdot \boldsymbol{\delta} \\ {}^T\delta_y = \mathbf{o} \cdot \boldsymbol{\delta} \\ {}^T\delta_z = \mathbf{a} \cdot \boldsymbol{\delta} \end{cases} \tag{19}$$

The above equations can be extended to the transformation of differential motion between any two reference frames:

$${}^T\mathbf{M} = {}^{T\mathbf{M}}\boldsymbol{J}_{\mathbf{M}} \cdot \mathbf{M} \tag{20}$$

where, ${}^{T\mathbf{M}}\boldsymbol{J}_{\mathbf{M}}$ is shown in the Appendix C, and the reference frame {**T**} is the transformation matrix between the two reference frames.

Next, the Jacobi matrix of RR-RP-RR manipulator is analyzed. The motion equation $\mathbf{x} = \mathbf{x}(\mathbf{q})$ of the manipulator shows the displacement relationship between the end space $\mathbf{x}$ and the joint space $\mathbf{q}$ of the manipulator. The differential motion of $\mathbf{x}$ is $\mathbf{M} = [\mathbf{d}, \quad \boldsymbol{\delta}]^T$, where $\mathbf{d}$ is the differential translation vector and $\boldsymbol{\delta}$ is the differential rotation vector. The above motion equation is derived from time t, that is $\dot{\mathbf{x}} = \boldsymbol{J}(\mathbf{q})\dot{\mathbf{q}}$, where $\dot{\mathbf{x}}$ is the generalized velocity for the end of manipulator, $\dot{\mathbf{q}}$ is the joint velocity, and $\boldsymbol{J}(\mathbf{q})$ is the Jacobi matrix of the manipulator. The generalized velocity $\dot{\mathbf{x}}$ consists of translation velocity $\mathbf{v}$ and angular velocity $\boldsymbol{\omega}$:

$$[\mathbf{v}, \quad \boldsymbol{\omega}] = \boldsymbol{J}(\mathbf{q})[\dot{q}_1, \ \cdots, \ \dot{q}_6]^T \tag{21}$$

Obviously, $\boldsymbol{J}(\mathbf{q})$ is a 6×6 square matrix, where $\boldsymbol{J}(\mathbf{q})(1,:)$, $\boldsymbol{J}(\mathbf{q})(2,:)$ and$\boldsymbol{J}(\mathbf{q})(3,:)$ show the linear transformation of the translation velocity $\mathbf{v}$, $\boldsymbol{J}(\mathbf{q})(4,:)$,$\boldsymbol{J}(\mathbf{q})(5,:)$ and $\boldsymbol{J}(\mathbf{q})(6,:)$ show the linear transformation of the angular velocity $\boldsymbol{\omega}$.

Therefore, the Jacobi matrix $\boldsymbol{J}(\mathbf{q})$ can be written as follows:

$$\boldsymbol{J}(\mathbf{q}) = \begin{bmatrix} \boldsymbol{J}_{d1} & \boldsymbol{J}_{d2} \cdots \boldsymbol{J}_{d6} \\ \boldsymbol{J}_{\delta 1} & \boldsymbol{J}_{\delta 2} \cdots \boldsymbol{J}_{\delta 6} \end{bmatrix} \tag{22}$$

where, each column vector$\boldsymbol{J}(\mathbf{q})(:,i) = [\boldsymbol{J}_{di} \quad \boldsymbol{J}_{\delta i}]^T$ represents the mapping relationship between joint velocity $\dot{q}_i$ and the generalized velocity for the end of manipulator,

$(i = 1, \cdots, 6)$.

The Jacobi matrix $\boldsymbol{J}(\mathbf{q})$ is solved using the differential transformation method.

The expression of the generalized velocity $\dot{\mathbf{x}}$ is as follows:

$$\dot{\mathbf{x}} = \lim_{\Delta t \to 0} \frac{1}{\Delta t} \begin{bmatrix} \mathbf{d} \\ \boldsymbol{\delta} \end{bmatrix} = \begin{bmatrix} \mathbf{v} \\ \boldsymbol{\omega} \end{bmatrix} \tag{23}$$

The above equation can be transformed into:

$$\mathbf{M} = \begin{bmatrix} \mathbf{d} \\ \boldsymbol{\delta} \end{bmatrix} = \lim_{\Delta t \to 0} \dot{\mathbf{x}} \Delta t \tag{24}$$

Substituting equation $\dot{\mathbf{x}} = \boldsymbol{J}(\mathbf{q})\dot{\mathbf{q}}$ into equation (24), it follows that

$$\mathbf{M} = \boldsymbol{J}(\mathbf{q})\, d\mathbf{q} \tag{25}$$

As shown in Figure 5, the axis z_i of the reference frames at each joint is along the direction of the joint axis. When the Jacobi matrix is constructed, the influence of the rotating joint and the translational joint is different.

The rotating joint k makes differential rotation $d\theta_k$ around the axis z_k, then the differential motion of joint k is obtained: $\mathbf{M} = [0 \quad 0 \quad 0 \quad 0 \quad 0 \quad d\theta_k]^T$.

It can be determined by means of equation (B.3) :

$${}^T\mathbf{M} = \left[(\mathbf{p} \times \mathbf{n})_z \quad (\mathbf{p} \times \mathbf{o})_z \quad (\mathbf{p} \times \mathbf{a})_z \quad n_z \quad o_z \quad a_z\right]^T \cdot d\theta_k \tag{26}$$

Where $[(\mathbf{p} \times \mathbf{n})_z \quad (\mathbf{p} \times \mathbf{o})_z \quad (\mathbf{p} \times \mathbf{a})_z \quad n_z \quad o_z \quad a_z]^T$ is column k of $\boldsymbol{J}(\mathbf{q})$.

The translational joint j makes differential translation dd_j around the axis z_j, then the differential motion of joint j is obtained: $\mathbf{M} = [0 \quad 0 \quad dd_j \quad 0 \quad 0 \quad 0]^T$.

It can be determined by means of equation (B.3) :

$${}^T\mathbf{M} = [n_z \quad o_z \quad a_z \quad 0 \quad 0 \quad 0]^T \cdot dd_j \tag{27}$$

Where $[n_z \quad o_z \quad a_z \quad 0 \quad 0 \quad 0]^T$ is column j of $\boldsymbol{J}(\mathbf{q})$.

For the RR-RP-RR manipulator, the transformation matrices ${}^1_6\mathbf{T}$, ${}^2_6\mathbf{T}$, ${}^3_6\mathbf{T}$, ${}^4_6\mathbf{T}$, ${}^5_6\mathbf{T}$ and ${}^6_6\mathbf{T}$ from each joint to the end joint are calculated according to the transformation matrix${}_n{}^{n-1}\mathbf{T}(n = 1, \cdots, 6)$ between adjacent joints. The column elements of $\boldsymbol{J}(\mathbf{q})$ can be computed by means of equations (26) and (27), that is, $\boldsymbol{J}(\mathbf{q})(:,i)$ can be obtained from the elements of matrix ${}^i_6\mathbf{T}(i = 1, \cdots, 6)$. Because ${}^i_6\mathbf{T}$ is only related to the configuration of the parallel manipulator, the expressions derived in this contribution for solving the velocity analysis do not require the calculation of the values of the passive joint velocity of the studied parallel manipulator.

The Jacobi matrix of the RR-RP-RR manipulator is solved above, and the mapping relationship between the velocity for each joint of the limb and the end joint velocity of the limb is obtained. Finally, what needs to be solved is the mapping relationship between the generalized velocity for the mobile platform of parallel manipulator and the velocity for the active joint of the limb, that is, the Jacobi matrix of the whole manipulator. Next, the relationship between the generalized velocity of the mobile platform and the velocity at the end of the limb needs to be solved.

The pose of the mobile platform is represented as the vector $\mathbf{q} = [\mathbf{p}^T, \quad \mathbf{t}^T]^T$, while $\mathbf{p} = [X, \ Y, \ Z]^T$ represents the position vector and $\mathbf{t} = [\varphi, \ \theta, \ \psi]^T$ represents the posture vector.

The generalized velocity $\dot{\mathbf{q}}$ of the mobile platform in the general global reference frame is given as follows:

$$\dot{\mathbf{q}} = \left[\dot{\mathbf{p}}^T, \ \boldsymbol{\omega}^T\right]^T \tag{28}$$

In equation (28), obviously the angular velocity vector $\boldsymbol{\omega}$ is not equal to $\dot{\mathbf{t}}$, that is, $\dot{\mathbf{q}} \neq \dot{\mathbf{q}}_t = [\dot{\mathbf{p}}^T, \ \dot{\mathbf{t}}^T]^T$.And $\boldsymbol{\omega}$ can be represented via the angular velocity vector $\boldsymbol{\omega}_P$ in the general body reference frame:

$$\boldsymbol{\omega} = \mathbf{R} \cdot \boldsymbol{\omega}_P \tag{29}$$

Where, $\mathbf{R} = Rot(x,\varphi) \cdot Rot(y,\theta) \cdot Rot(z,\psi)$.

The following relationship exists between $\boldsymbol{\omega}_P$ and $\dot{\mathbf{t}}$

$$\boldsymbol{\omega}_p = \mathbf{E} \cdot \dot{\mathbf{t}} \tag{30}$$

Where,

$$\mathbf{E} = \begin{bmatrix} c\theta\, c\psi & s\psi & 0 \\ -c\theta\, s\psi & c\psi & 0 \\ s\theta & 0 & 1 \end{bmatrix}$$

Therefore, $\boldsymbol{\omega}$ can be represented using $\dot{\mathbf{t}}$:

$$\boldsymbol{\omega} = \mathbf{R} \cdot \mathbf{E} \cdot \dot{\mathbf{t}} \tag{31}$$

Equation(28) can be expressed as:

$$\dot{\mathbf{q}} = {}^{q}\mathbf{J}_{q_t} \begin{bmatrix} \dot{\mathbf{p}} \\ \dot{\mathbf{t}} \end{bmatrix} \tag{32}$$

Where, ${}^{q}\mathbf{J}_{q_t} = \begin{bmatrix} \mathbf{I}_{3\times3} & 0 \\ 0 & \boldsymbol{RE} \end{bmatrix}$.

The relationship between the differential motion for the end joint of the RR-RP-RR manipulator and the generalized differential motion of the mobile platform satisfies the equation (19). Therefore, if the generalized velocity $\dot{\mathbf{q}}$ of the mobile platform is known, the velocity $\dot{\mathbf{q}}_h$ of hinge points P_i can be obtained according to equation (20), as follows:

$$\dot{\mathbf{q}}_h = {}^{q_h}\mathbf{J}_{\mathbf{q}} \cdot \dot{\mathbf{q}} \tag{33}$$

${}^{q_h}\mathbf{J}_{\mathbf{q}}$ is determined by means of the transformation matrix ${}^{O_p}\mathbf{T}_{O_{6i}}$ between two reference frames.

Combining equations (26), (27), (33), the Jacobi matrix from the velocity for each limb joint to the generalized velocity of the mobile platform can be obtained:

$$\dot{\mathbf{q}} = \mathbf{J}_F \cdot \dot{\mathbf{q}}_j \tag{34}$$

where, $\mathbf{J}_F = {}^{q_h}\mathbf{J}_{\mathbf{q}}^{-1} \cdot \boldsymbol{J}(\mathbf{q})$, $\dot{\mathbf{q}}_j = [\dot{\theta}_1, \ \dot{\theta}_2, \ \dot{\theta}_3, \ \dot{L}_4, \ \dot{\theta}_5, \ \dot{\theta}_6]^T$.

Because the active joint of the RR-RP-RR manipulator is the prismatic joint, the Jacobi matrix for the parallel manipulator represents the mapping relationship between the generalized velocity of the mobile platform and the velocity for active joints of the six limbs.

$$\dot{\mathbf{q}}_{\mathbf{j}}(4) = \mathbf{J}_F^{-1}(4) \cdot \dot{\mathbf{q}} \tag{35}$$

Therefore, it can be computed:

$$\dot{\mathbf{L}} = \mathbf{J}_I \cdot \dot{\mathbf{q}} \tag{36}$$

Where $\dot{\mathbf{L}} = [\dot{L}_{41}, \ \dot{L}_{42}, \ \dot{L}_{43}, \ \dot{L}_{44}, \ \dot{L}_{45}, \ \dot{L}_{46}]^T$,

$\mathbf{J}_I = [\mathbf{J}_{F1}^{-1}(4), \ \mathbf{J}_{F2}^{-1}(4), \ \mathbf{J}_{F3}^{-1}(4), \ \mathbf{J}_{F4}^{-1}(4), \ \mathbf{J}_{F5}^{-1}(4), \ \mathbf{J}_{F6}^{-1}(4)]^T$.

From equation (36), $\dot{\mathbf{q}} = \mathbf{J} \cdot \dot{\mathbf{L}}$ can be obtained, and the Jacobi matrix of the whole manipulator is as follows:

$$\mathbf{J} = \mathbf{J}_I^{-1} \tag{37}$$

4.2. Acceleration analysis

In this section, the acceleration analysis of the parallel manipulator is carried out by means of the differential transformation method. The inverse acceleration analysis consists of computing the joint acceleration vector of the manipulator given the generalized acceleration of the mobile platform with respect to the fixed platform.

The generalized acceleration $\ddot{\mathbf{q}}$ of the mobile platform in the general global reference frame is given as follows:

Table 2.
Parameters of the parallel manipulator.

$R_P = 0.125m, \quad R_B = 0.160m$
$\theta_P = 24^\circ, \quad \theta_B = 96^\circ$
$U_{offset} = 0.01m$
$h = 0.295m, \quad h_P = 0.026m, \quad h_B = 0.027m$
$L_1 = 0.2899 + 0.008 \cdot \sin(0.25\pi t) \cdot \cos(0.25\pi t)$
$L_2 = 0.2899 + 0.018 \cdot \sin(0.25\pi t) \cdot \cos(0.25\pi t)$
$L_3 = 0.2899 + 0.004 \cdot \sin(0.25\pi t)$
$L_4 = 0.2899 + 0.013 \cdot \sin(0.25\pi t)$
$L_5 = 0.2899 - 0.03 \cdot \sin(0.25\pi t)$
$L_6 = 0.2899 + 0.02 \cdot \sin(0.25\pi t), \quad 0 \le t \le 8$

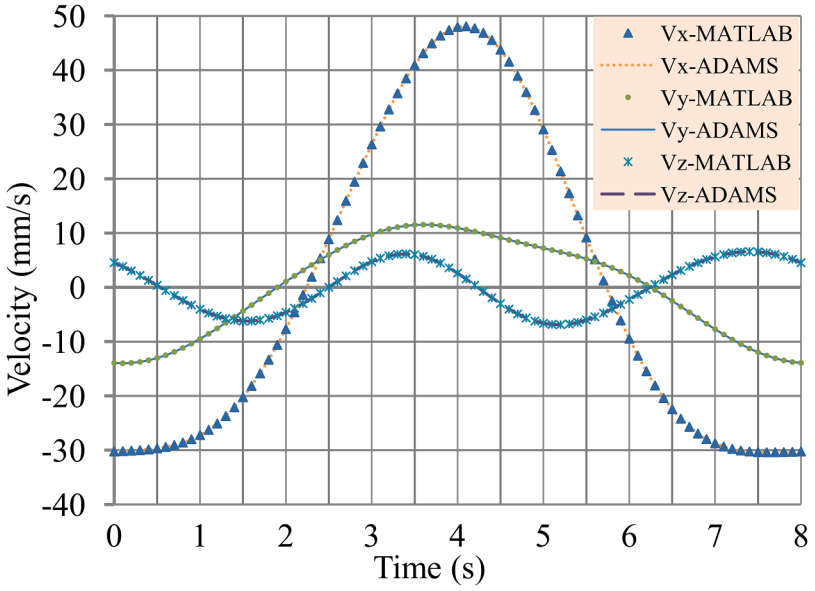

Fig. 7. Time history of the velocity of the center of the mobile platform.

$$\ddot{\mathbf{q}} = \left[\ddot{\mathbf{p}}^T, \quad \dot{\boldsymbol{\omega}}^T\right]^T \tag{38}$$

where, obviously the linear acceleration vector $\ddot{\mathbf{p}}$ can be obtained easily, but the angular acceleration vector $\dot{\boldsymbol{\omega}}$ is not equal to $\ddot{\mathbf{t}}$.

After the time derivative of Eq. (29) is obtained, the angular acceleration vector $\dot{\boldsymbol{\omega}}$ is computed as follows:

$$\dot{\boldsymbol{\omega}} = \dot{\mathbf{R}} \cdot \boldsymbol{\omega}_P + \mathbf{R} \cdot \dot{\boldsymbol{\omega}}_P \tag{39}$$

where $\dot{\mathbf{R}} = \mathbf{R} \cdot \widetilde{\boldsymbol{\omega}}_P$, $\widetilde{\boldsymbol{\omega}}_P$ is the skew symmetric matrix of $\boldsymbol{\omega}_P$.

The angular acceleration vector $\dot{\boldsymbol{\omega}}_P$ in the general body reference frame is then obtained using Eq. (30):

$$\dot{\boldsymbol{\omega}}_p = \dot{\mathbf{E}} \cdot \dot{\mathbf{t}} + \mathbf{E} \cdot \ddot{\mathbf{t}} \tag{40}$$

Combining equations (36), (38), (39), the relationship between the acceleration for the active joint of the limb and the generalized acceleration of the mobile platform can be obtained:

$$\ddot{\mathbf{L}} = \dot{\mathbf{J}}_I \cdot \dot{\mathbf{q}} + \mathbf{J}_I \cdot \ddot{\mathbf{q}} \tag{41}$$

By means of equations (36) and (37), the generalized acceleration of the mobile platform is computed:

$$\ddot{\mathbf{q}} = \dot{\mathbf{J}} \cdot \dot{\mathbf{L}} + \mathbf{J} \cdot \ddot{\mathbf{L}} \tag{42}$$

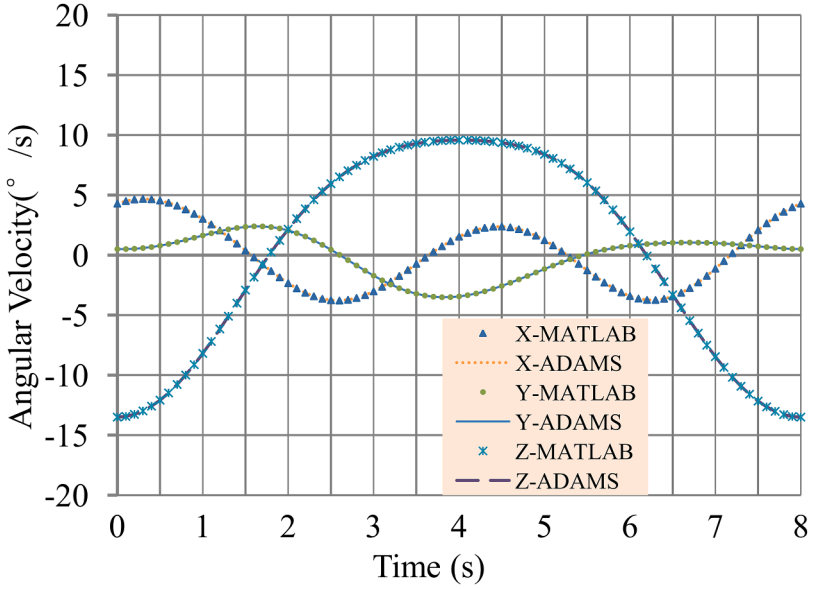

Fig. 8. Time history of the angular velocity of the mobile platform.

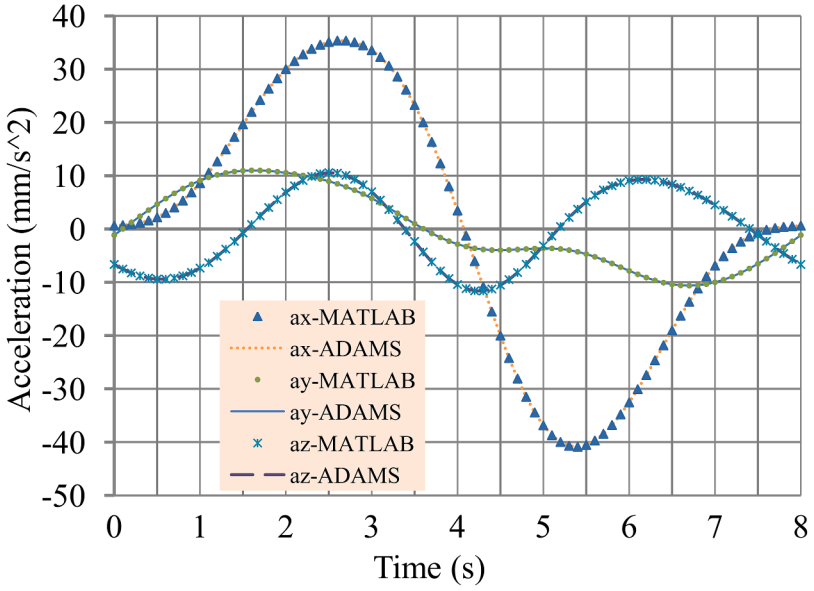

Fig. 9. Time history of the acceleration of the center of the mobile platform.

5. Case study

In order to verify the effectiveness of the method presented in this research to solve the kinematics of 6-RR-RP-RR parallel manipulator, a numerical example is given in this section. Table 2 shows the configuration parameters. Numerical analysis needs to calculate the forward kinematics analysis by giving six limbs lengths. Therefore, the generalized coordinates L_i $(i = 1,\ 2, \cdots, 6)$ of six limbs lengths are given in Table 2, and the velocity, angular velocity, acceleration and angular acceleration of the mobile platform with respect to the fixed platform are calculated.

The generalized coordinates of the limb lengths are controlled by periodical functions, and the unit is meter. The parallel manipulator begins its motion from the zero position at the time $t = 0$ and returns to its original configuration after 8 s. The time history of the velocity and acceleration of the mobile platform with respect to the fixed platform is shown in Figs. 7 -10. Finally, in order to verify the kinematics formula of the parallel manipulator based on the differential transformation method and D-H parameter method,

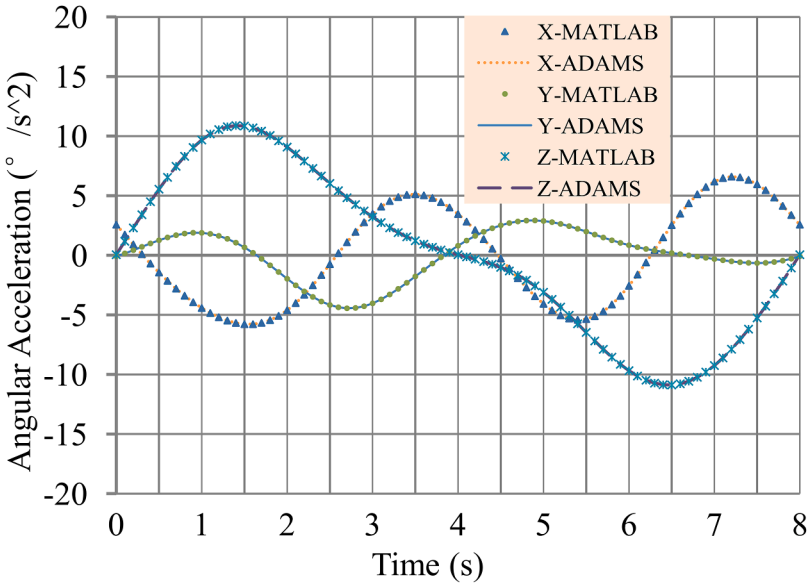

Fig. 10. Time history of the angular acceleration of the mobile platform.

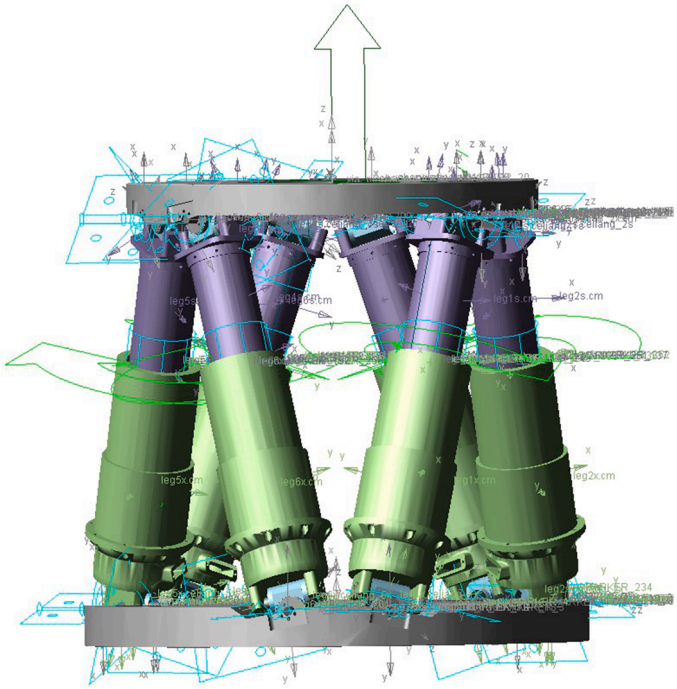

Fig. 11. The ADAMS model for the studied parallel manipulator.

the simulation software ADAMS is used to determine the velocity and acceleration of the mobile platform. The ADAMS model for the studied parallel manipulator is shown in Fig. 11. The simulation results obtained are provided in Figs. 7 - 10. Referring to the results in Figs. 7 - 10, the numerical solutions obtained via the differential transformation method are in excellent agreement with the results obtained using the simulation model in ADAMS, proving the efficacy of the proposed method.

6. Conclusion

In this work, the displacement, velocity and acceleration of a Gough-Stewart parallel manipulator with special structure, known as

6-RR-RP-RR parallel manipulator, are analyzed by means of Denavit-Hartenberg method and differential transformation method. Limited workspace is a drawback of a general Gough-Stewart platform, and offset hinges can improve its workspace. The positive impact of the offset hinge on the workspace is verified by an example. The 6-RR-RP-RR parallel manipulator studied in this article, in addition to the application in the secondary mirror or the third-mirror adjustment system of large-aperture telescopes, has potential applications including precision positioning of surgical manipulators and pointing devices, dynamic tracking of targeting systems. Compared with a general Gough-Stewart platform, the limbs of the manipulator are connected to the mobile and fixed platforms through offset hinges. Meanwhile, the introduction of hinge offset variable makes its kinematics more complicated and difficult to solve effectively. The traditional kinematics modeling method for parallel manipulator can not be used to analyze the kinematics of the parallel manipulator studied. The hinge constraint algorithm proposed in reference [47–49] has great limitations, and can only solve the displacement relationship through the complex modeling process. In this contribution, the kinematics of 6-RR-RP-RR parallel manipulator with offset hinges is approached successfully by the means of the hybrid method combining Denavit-Hartenberg method and differential transformation method. As far as the authors are aware, the velocity and acceleration analysis of the 6-RR-RP-RR parallel manipulator using offset hinges has not been reported in previous work. The derivation of acceleration analysis of the 6-RR-RP-RR parallel manipulator using the hybrid approach is novel in this research field. As an intermediate step, this contribution also provides the forward and inverse displacement analysis. Simple and compact expressions of velocity and acceleration can be easily translated into computer programs. The expressions derived in this contribution for solving the acceleration analysis do not require the calculation of the values of the passive joint acceleration of the studied parallel manipulator. In order to prove the versatility of the expressions obtained by the hybrid method in solving the kinematics of the parallel manipulator, up to the acceleration analysis, a numerical example was provided and verified with the help of the simulation software. According to the Figs. 7 - 10, the numerical solutions obtained via the hybrid method are in excellent agreement with the results obtained using the simulation model in ADAMS, proving the efficacy of the proposed method.

The hybrid method and formulas derived in this study are general, universal and continuous. They can be applied to kinematic analysis for other complex parallel manipulators as well. Based on the velocity and acceleration expressions, future work will focus on the dynamics and control strategy of such parallel manipulator.

Declaration of Competing Interest

The authors declare that they have no known competing financial interests or personal relationships that could have appeared to influence the work reported in this paper.

Acknowledgments

This work was supported by the National Natural Science Foundation of China [Grant No. 52005478] and Jilin Scientific and Technological Development Program [20200404204YY].

Appendix A

The kinematic equations can be established via Eq. (9):

$$\left.\begin{aligned}
n_x &= -c6\cdot(c5\cdot(s1\cdot s3 - c1\cdot c2\cdot c3) + c1\cdot s2\cdot s5) - s6\cdot(s1\cdot c3 + c1\cdot c2\cdot s3)\\
n_y &= c6\cdot(c5\cdot(c1\cdot s3 + s1\cdot c2\cdot c3) - s1\cdot s2\cdot s5) + s6\cdot(c1\cdot c3 - s1\cdot c2\cdot s3)\\
n_z &= c6\cdot(c2\cdot c5 + s2\cdot c3\cdot c5) - s2\cdot s3\cdot s6\\
r_x &= s6\cdot(c5\cdot(s1\cdot s3 - c1\cdot c2\cdot c3) + c1\cdot s2\cdot s5) - c6\cdot(s1\cdot c3 + c1\cdot c2\cdot s3)\\
r_y &= c6\cdot(c1\cdot c3 - s1\cdot c2\cdot s3) - s6\cdot(c5\cdot(c1\cdot s3 + s1\cdot c2\cdot c3) - s1\cdot s2\cdot s5)\\
r_z &= -s6\cdot(c2\cdot s5 + s2\cdot c3\cdot c5) - s2\cdot s3\cdot c6\\
a_x &= s5\cdot(s1\cdot s3 - c1\cdot c2\cdot c3) - c1\cdot s2\cdot c5\\
a_y &= -s5\cdot(c1\cdot s3 + s1\cdot c2\cdot c3) - s1\cdot s2\cdot c5\\
a_z &= c2\cdot c5 - s2\cdot c3\cdot s5\\
p_x &= U_{offset}\cdot c1 - U_{offset}\cdot(c5\cdot(s1\cdot s3 - c1\cdot c2\cdot c3) + c1\cdot s2\cdot s5) - L_{4i}\cdot c1\cdot s2)\\
p_y &= U_{offset}\cdot s1 + U_{offset}\cdot(c5\cdot(c1\cdot s3 + s1\cdot c2\cdot c3) - s1\cdot s2\cdot s5) - L_{4i}\cdot s1\cdot s2)\\
p_z &= U_{offset}\cdot(c2\cdot s5 + s2\cdot c3\cdot c5) + L_{4i}\cdot c2)
\end{aligned}\right\}$$

where, $c(m) = \cos(\theta_{mi})$, $s(m) = \sin(\theta_{mi})$, $(m = 1, 2, 3, 5, 6)$.

Appendix B

The rotation transformation matrix when any reference frame rotates angle θ around any vector **f** starting from the origin is as follows:

$$Rot(\mathbf{f},\ \theta)=\begin{bmatrix} f_xf_xvers\theta+c\theta & f_yf_xvers\theta-f_zs\theta & f_zf_xvers\theta+f_ys\theta & 0\\ f_xf_yvers\theta+f_zs\theta & f_yf_yvers\theta+c\theta & f_zf_yvers\theta-f_xs\theta & 0\\ f_xf_zvers\theta-f_ys\theta & f_yf_zvers\theta+f_xs\theta & f_zf_zvers\theta+c\theta & 0\\ 0 & 0 & 0 & 1\end{bmatrix} \tag{B.1}$$

where, $s\theta=\sin(\theta)$, $c\theta=\cos(\theta)$, $vers\theta=1-\cos(\theta)$, f_x, f_y, f_z are the components of vector $\mathbf{f}$ on the three coordinate axes of the reference frame.

For the differential motion $d\theta$, substituting $\lim_{\theta\to0} s\theta=d\theta$, $\lim_{\theta\to0} c\theta=1$, $\lim_{\theta\to0} vers\theta=0$ into equation (B.1), it can be obtained that:

$$Rot(\mathbf{f},\ d\theta)=\begin{bmatrix} 1 & -f_zd\theta & f_yd\theta & 0\\ f_zd\theta & 1 & -f_xd\theta & 0\\ -f_yd\theta & f_xd\theta & 1 & 0\\ 0 & 0 & 0 & 1\end{bmatrix} \tag{B.2}$$

Substituting $f_xd\theta=\delta_x$, $f_yd\theta=\delta_y$, $f_zd\theta=\delta_z$ into $\Delta=Trans(d_x,d_y,d_z)Rot(\mathbf{f},\ d\theta)-I$, the differential transformation operator Δ may be expressed as follows:

$$\Delta=\begin{bmatrix}1&0&0&d_x\\0&1&0&d_y\\0&0&1&d_z\\0&0&0&1\end{bmatrix}\bullet\begin{bmatrix}1&-\delta_z&\delta_y&0\\\delta_z&1&-\delta_x&0\\-\delta_y&\delta_x&1&0\\0&0&0&1\end{bmatrix}-\begin{bmatrix}1&0&0&0\\0&1&0&0\\0&0&1&0\\0&0&0&1\end{bmatrix}=\begin{bmatrix}0&-\delta_z&\delta_y&d_x\\\delta_z&0&-\delta_x&d_x\\-\delta_y&\delta_x&0&d_x\\0&0&0&0\end{bmatrix} \tag{B.3}$$

Appendix C

When differential motions of the two reference frames are equal, the equation $\Delta\cdot\mathbf{T}=\mathbf{T}\cdot{}^T\Delta$ can be obtained. It is evident that:

$$\mathbf{T}^{-1}\cdot\Delta\cdot\mathbf{T}={}^T\Delta \tag{C.1}$$

The left side of equation (C.1) can be expressed as follows:

$$\mathbf{T}^{-1}\cdot\Delta\cdot\mathbf{T}=\begin{bmatrix}n_x&o_x&a_x&p_x\\n_y&o_y&a_y&p_y\\n_z&o_z&a_z&p_z\\0&0&0&1\end{bmatrix}^{-1}\bullet\begin{bmatrix}0&-\delta_z&\delta_y&d_x\\\delta_z&0&-\delta_x&d_y\\-\delta_y&\delta_x&0&d_z\\0&0&0&0\end{bmatrix}\bullet\begin{bmatrix}n_x&o_x&a_x&p_x\\n_y&o_y&a_y&p_y\\n_z&o_z&a_z&p_z\\0&0&0&1\end{bmatrix} \tag{C.2}$$

It follows that:

$${}^T\Delta=\begin{bmatrix}0&-\boldsymbol{\delta}\cdot\mathbf{a}&\boldsymbol{\delta}\cdot\mathbf{o}&\boldsymbol{\delta}\cdot(\mathbf{p}\times\mathbf{n})+\mathbf{d}\cdot\mathbf{n}\\\boldsymbol{\delta}\cdot\mathbf{a}&0&-\boldsymbol{\delta}\cdot\mathbf{n}&\boldsymbol{\delta}\cdot(\mathbf{p}\times\mathbf{o})+\mathbf{d}\cdot\mathbf{o}\\-\boldsymbol{\delta}\cdot\mathbf{o}&\boldsymbol{\delta}\cdot\mathbf{n}&0&\boldsymbol{\delta}\cdot(\mathbf{p}\times\mathbf{a})+\mathbf{d}\cdot\mathbf{a}\\0&0&0&0\end{bmatrix} \tag{C.3}$$

Therefore, via the equivalence between equation (13) and equation (15), the relationship between two differential motions ${}^T\mathbf{M}$ and $\mathbf{M}$ can be obtained:

$$\begin{bmatrix}{}^Td_x\\{}^Td_y\\{}^Td_z\\{}^T\delta_x\\{}^T\delta_y\\{}^T\delta_z\end{bmatrix}={}^{T\mathbf{M}}\boldsymbol{J}_{\mathbf{M}}\bullet\begin{bmatrix}d_x\\d_y\\d_z\\\delta_x\\\delta_y\\\delta_z\end{bmatrix} \tag{C.4}$$

where, ${}^{T\mathbf{M}}\boldsymbol{J}_{\mathbf{M}}=\begin{bmatrix}n_x&n_y&n_z&(\mathbf{p}\times\mathbf{n})_x&(\mathbf{p}\times\mathbf{n})_y&(\mathbf{p}\times\mathbf{n})_z\\o_x&o_y&o_z&(\mathbf{p}\times\mathbf{o})_x&(\mathbf{p}\times\mathbf{o})_y&(\mathbf{p}\times\mathbf{o})_z\\a_x&a_y&a_z&(\mathbf{p}\times\mathbf{a})_x&(\mathbf{p}\times\mathbf{a})_y&(\mathbf{p}\times\mathbf{a})_z\\0&0&0&n_x&n_y&n_z\\0&0&0&o_x&o_y&o_z\\0&0&0&a_x&a_y&a_z\end{bmatrix}$

References

[1] V.E. Gough, Contribution to discussion of papers on research in automobile stability, in, in: Proceedings of the Automobile Division of the Institution of Mechanical Engineers, New York, 1957, pp. 392–394.
[2] V.E. Gough, S.G. Whitehall, Universal tyre testing machine, in: Proceedings of the 9th International Automobile Technical Congress, 1962, pp. 117–137.
[3] D. Stewart, A platform with six degrees of freedom, in: Proceedings of the Institution of Mechanical Engineers, 1965, pp. 371–386.
[4] D. Stewart, A platform with six degrees of freedom: a new form of mechanical linkage which enables a platform to move simultaneously in all six degrees of freedom developed by Elliott-automation, Aircr. Eng. Aerospatial Technol. 38 (4) (1966) 30–35, https://doi.org/10.1108/eb034141. Apr.
[5] W. Dong, Z.J. Du, Y.Q. Xiao, X.G. Chen, Development of a parallel kinematic motion simulator platform, Mechatronics 23 (1) (2013) 154–161, https://doi.org/10.1016/j.mechatronics.2012.10.004. Feb.
[6] K. Yamane, Y. Nakamura, M. Okada, N. Komine, K. Yoshimoto, Parallel dynamics computation and H_{∞}infinity acceleration control of parallel manipulators for acceleration display, J. Dyn. Syst. Meas. Control 127 (2) (Jun. 2005) 185–191, https://doi.org/10.1115/1.1898229.
[7] P. Ngoc, J.H. Kim, H.S. Kim, Development of a new 6-DOF parallel-kinematic motion simulator, in: Proceedings of the International Conference on Control, Automation and Systems, Seoul, Korea, 2008, pp. 2370–2373, https://doi.org/10.1109/ICCAS.2008.4694202.
[8] R. Cao, F. Gao, Y. Zhang, D.L. Pan, W.X. Chen, A new parameter design method of a 6-DOF parallel motion simulator for a given workspace, Mech. Based Des. Struct. Mach. 43 (1) (2014) 1–18, https://doi.org/10.1080/15397734.2014.904234. Sep.
[9] D.S. Wu, H.B. Gu, P. Li, Comparative study on dynamic identification of parallel motion platform for a novel flight simulator, in: Proceedings of the IEEE International Conference on Robotics and Biomimetics, Guilin, China, 2009, pp. 2232–2237.
[10] F.R. Bi, T. Ma, X. Wang, X. Yang, Z.P. Lv, Research on vibration control of seating system platform based on the cubic stewart parallel mechanism, IEEE Access 7 (2019) 155637–155649, https://doi.org/10.1109/ACCESS.2019.2948785. Oct.
[11] A. Preumont, M. Horodinca, I. Romanescu, B. de Marneffe, M. Avraam, A. Deraemaeker, F. Bossens, A.Abu Hanieh, 'A six-axis single-stage active vibration isolator based on Stewart platform, J. Sound Vib. 300 (3-5) (Mar. 2007) 644–661, https://doi.org/10.1016/j.jsv.2006.07.050.
[12] J.F. Yang, Z.B. Xu, Q.W. Wu, Z.S. Wang, H. Li, S. He, Design of a vibration isolation system for the space telescope, J. Guid. Control Dyn. 38 (12) (2015) 2441–2448, https://doi.org/10.2514/1.G001221. Apr.
[13] D.R. Neill, R. Sneed, J. Dawson, J. Sebag, W. Gressler, Baseline design and requirements for the LSST hexapod and rotator, in: Proceedings of the SPIE 9151, Advances in Optical and Mechanical Technologies for Telescopes and Instrumentation, Montréal, Quebec, Canada, 2014, 91512B1-91512B16.
[14] R.C. Sneed, M.F. Cash, T.S. Chambers, P.C. Janzen, Six degrees of freedom, sub-micrometer positioning system for secondary mirrors, in: Procedings of the SPIE 7733, Ground-based and Airborne Telescopes III, San Diego, California, United States, 2010, https://doi.org/10.1117/12.857793, 77332R1-77332R11.
[15] J. Rousselle, K. Byrum, R. Cameron, et al., Toward the construction of a medium size prototype schwarzschild-couder telescope for CTA, in: Procedings of the SPIE 9603, Optics for EUV, X-Ray, and Gamma-Ray Astronomy VII, San Diego, California, United States, 2015, https://doi.org/10.1117/12.2188381, 960305-1-960305-12.
[16] Z.Y. Jia, S. Lin, W. Liu, Measurement method of six-axis load sharing based on the Stewart platform, Measurement 43 (3) (2010) 329–335, https://doi.org/10.1016/j.measurement.2009.11.005. Apr.
[17] Y.L. Hou, D.X. Zeng, J.T. Yao, K.J. Kang, L. Lu, Y.S. Zhao, Optimal design of a hyperstatic Stewart platform-based force/torque sensor with genetic algorithms, Mechatronics 19 (2) (2009) 199–204, https://doi.org/10.1016/j.mechatronics.2008.08.002. Mar.
[18] R. Ranganath, P.S. Nair, T.S. Mruthyunjaya, A. Ghosal, A force/torque sensor based on a Stewart platform in a near-singular configuration, Mech. Mach. Theory 39 (9) (2004) 971–998, https://doi.org/10.1016/j.mechmachtheory.2004.04.005. Sep.
[19] S. Qian, B. Zi, D.M. Wang, Y. Li, Development of modular cable-driven parallel robotic systems, IEEE Access 7 (2018) 5541–5553, https://doi.org/10.1109/ACCESS.2018.2889245. Dec.
[20] H. Ji, W.W. Shang and S. Cong, "Adaptive synchronization control of cable-driven parallel robots with uncertain kinematics and dynamics," IEEE Trans. Ind. Electron., to be published. 10.1109/TIE.2020.3013776.
[21] F. Gao, B.B. Peng, H. Zhao, W.M. Li, A novel 5-DOF fully parallel kinematic machine tool, Int. J. Adv. Manuf. Technol. 31 (1-2) (2006) 201–207, https://doi.org/10.1007/s00170-005-0171-1. Mar.
[22] Y. Lu, J.Y. Xu, Simulation of three-dimensional free-form surface normal machining by 3SPS+RRPU and 2SPS+RRPRR parallel machine tools, Proc. Inst. Mech. Eng. Part B J. Eng. Manuf. 222 (4) (2008) 485–494, https://doi.org/10.1243/09544054JEM900. Jun.
[23] F.G. Xie, X.J. Liu, X. Luo, M. Wabner, Mobility, singularity, and kinematics analyses of a novel spatial parallel mechanism, J. Mech. Robot. 8 (6) (2016), https://doi.org/10.1115/1.4034886, 061022-1-061022-10Dec.
[24] Y.J. Wang, B. Belzile, J. Angeles, Q.C. Li, Kinematic analysis and optimum design of a novel 2PUR-2RPU parallel robot, Mech. Mach. Theory 139 (2019) 407–423, https://doi.org/10.1016/j.mechmachtheory.2019.05.008. Sep.
[25] B.B. Lian, T. Sun, Y.M. Song, Y. Jin, M. Price, Stiffness analysis and experiment of a novel 5-DoF parallel kinematic machine considering gravitational effects, Int. J. Mach. Tools Manuf. 95 (Aug. 2015) 82–96, https://doi.org/10.1016/j.ijmachtools.2015.04.012.
[26] D. Deblaise, X. Hernot, P. Maurine, A systematic analytical method for PKM stiffness matrix calculation, in: Proceedings of the 2006 IEEE International Conference on Robotics and Automation, Florida, USA, 2006, pp. 4213–4219.
[27] R.Y. Zhao, L.L. Wu, Y.H. Chen, Robust control for nonlinear delta parallel robot with uncertainty: an online estimation approach, IEEE Access 8 (2020) 97604–97617, https://doi.org/10.1109/ACCESS.2020.2997093. May.
[28] D.Y. Shang, Y. Li, Y. Liu, S.W. Cui, Research on the motion error analysis and compensation strategy of the Delta robot, Mathematics 7 (5) (2019) 411, https://doi.org/10.3390/math7050411. May.
[29] G. Aquino, J.D.J. Rubio, J. Pacheco, et al., Novel nonlinear hypothesis for the delta parallel robot modeling, IEEE Access 8 (2020) 46324–46334, https://doi.org/10.1109/ACCESS.2020.2979141. Mar.
[30] S.M. Kim, B.J. Yi, J.H.Chung Chung, J. Cheong, W. Kim, Development of a new neurosurgical 5-DOF parallel robot for stereotactic DBS operations, Int. J. Precis. Eng. Manuf. 18 (3) (2017) 333–343, https://doi.org/10.1007/s12541-017-0041-4. Mar.
[31] T. Essomba, Y. Hsu, J.S.S. Arevalo, M.A. Laribi, S. Zeghloul, Kinematic optimization of a reconfigurable spherical parallel mechanism for robotic-assisted craniotomy, J. Mech. Robot. 11 (6) (2019), 060905, https://doi.org/10.1115/1.4044411. Dec.
[32] J. Gallardo-Alvarado, J.M. Rico-Martínez, G. Alici, Kinematics and singularity analyses of a 4-dof parallel manipulator using screw theory, Mech. Mach. Theory 41 (9) (2006) 1048–1061, https://doi.org/10.1016/j.mechmachtheory.2005.10.012. Sep.
[33] J. Gallardo-Alvarado, A. Ramírez-Agundis, H. Rojas-Garduño, B. Arroyo- Ramírez, Kinematics of an asymmetrical three-legged parallel manipulator by means of the screw theory, Mech. Mach. Theory 45 (7) (2010) 1013–1023, https://doi.org/10.1016/j.mechmachtheory.2010.02.003. Jul.
[34] J. Gallardo-Alvarado, H. Orozco-Mendoza, A. Maeda-Sánchez, Acceleration and singularity analyses of a parallel manipulator with a particular topology, Meccanica 42 (3) (2007) 223–238, https://doi.org/10.1007/s11012-006-9042-6. Feb.
[35] Y.L. Liu, H.T. Wu, Y.X. Yang, S.Y. Zou, X.X. Zhang, Y.Y. Wang, Symmetrical workspace of 6-UPS parallel robot using tilt and torsion angles, Math. Probl. Eng. 6 (2018) 1–10, https://doi.org/10.1155/2018/6412030. Jun.
[36] P.D. Wu, H.G. Xiong, J.Y. Kong, Dynamic analysis of 6-SPS parallel mechanism, Int. J. Mech. Mater. Des. 8 (2012) 121–128, https://doi.org/10.1007/s10999-012-9181-y. Jun.
[37] G.J. Liu, Z.Y. Qu, X.C. Liu, et al., Singularity analysis and detection of 6-UCU parallel manipulator, Robot. Comput. Integr. Manuf. 30 (2) (2014) 172–179, https://doi.org/10.1016/j.rcim.2013.09.010. Apr.
[38] M. Raghavan, The Stewart platform of general geometry has 40 configurations, J. Mech. Des. 115 (2) (1993) 277–282, https://doi.org/10.1115/1.2919188. Jun.
[39] M.L. Husty, An algorithm for solving the direct kinematics of general Stewart- Gough platforms, Mech. Mach. Theory 31 (4) (1996) 365–379, https://doi.org/10.1016/0094-114X(95)00091-C. May.

[40] L. Rolland, Certified solving of the forward kinematics problem with an exact algebraic method for the general parallel manipulator, Adv. Robot. 19 (9) (2005) 995–1025, https://doi.org/10.1163/156855305774307004.
[41] J. Gallardo-Alvarado, A simple method to solve the forward displacement analysis of the general six-legged parallel manipulator, Robot. Comput. Integr. Manuf. 30 (1) (2014) 55–61, https://doi.org/10.1016/j.rcim.2013.09.001. Feb.
[42] D.M. Gan, Q.Z. Liao, J.S. Dai, S.M. Wei, L.D. Seneviratne, Forward displacement analysis of the general 6-6 Stewart mechanism using Gröbner bases, Mech. Mach. Theory 44 (9) (2009) 1640–1647, https://doi.org/10.1016/j.mechmachtheory.2009.01.008. Sep.
[43] X.G. Huang, Q.Z. Liao, S.M. Wei, Closed-form forward kinematics for a symmetrical 6-6 Stewart platform using algebraic elimination, Mech. Mach. Theory 45 (2) (2010) 327–334, https://doi.org/10.1016/j.mechmachtheory.2009.09.008. Feb.
[44] B. Hu, Y. Lu, Analyses of kinematics, statics, and workspace of a 3-RRPRR parallel manipulator and its three isomeric mechanisms, Proc. Inst. Mech. Eng. Part C J. Mech. Eng. Sci. 222 (9) (2008) 1829–1837, https://doi.org/10.1243/09544062JMES928. Sep.
[45] R. Gloess, B. Lula, Challenges of extreme load hexapod design and modularization for large ground-based telescopes, in: Proceedings of the SPIE, Modern Technologies in Space- and Ground-based Telescopes and Instrumentation 7739, 2010, pp. 327–330, https://doi.org/10.1117/12.858156. Jul.
[46] K. Großmann, B. Kauschinger, Eccentric universal joints for parallel kinematic machine tools: variants and kinematic transformations, Prod. Eng. Res. Dev. 6 (2012) 521–529, https://doi.org/10.1007/s11740-012-0405-7. Jul.
[47] M.M. Dalvand, B. Shirinzadeh, Forward kinematics analysis of offset 6-RRCRR parallel manipulators, Proc. Inst. Mech. Eng. Part C J. Mech. Eng. Sci. 225 (12) (2011) 3011–3018, https://doi.org/10.1177/0954406211411249. Sep.
[48] M.M. Dalvand, B. Shirinzadeh, Kinematics analysis of 6-DOF parallel micro-manipulators with offset U-joints: a case study, Int. J. Intell. Mechatron. Robot. 2 (1) (2012) 28–40, https://doi.org/10.4018/ijimr.2012010102. Jan.
[49] Y. Yu, Z.B. Xu, Q.W. Wu, P. Yu, S. He, G.Q. Wang, Kinematic analysis and testing of a 6-RRRPRR parallel manipulator, Proc. Inst. Mech. Eng. Part C J. Mech. Eng. Sci. 231 (13) (2016) 2515–2527, https://doi.org/10.1177/0954406216633034. Feb.
[50] H.S.A.Q.E. Han, C.Y. Han, Z.B. Xu, M.C. Zhu, Y. Yu, Q.W. Wu, Kinematics analysis and testing of novel 6-P-RR-R-RR parallel platform with offset RR-joints, Proc. Inst. Mech. Eng. Part C J. Mech. Eng. Sci. 233 (10) (2019) 3512–3530, https://doi.org/10.1177/0954406218817001. May.
[51] G.Q. Zhang, J.J. Du, S. To, Study of the workspace of a class of universal joints, Mech. Mach. Theory 73 (2) (2014) 244–258, https://doi.org/10.1016/j.mechmachtheory.2013.11.004. Mar.
[52] X.J. Liu, C. Wu, J.S. Wang, A new approach for singularity analysis and closeness measurement to singularities of parallel manipulators, J. Mech. Robot. 4 (4) (2012), https://doi.org/10.1115/1.4007004, 041001-1-041001-10Nov.